servations support our assertion that the stable[31] solid-state voltammogram of Figure 7A corresponds to the production of Fe(III/III) at one Pt finger and Fe(II/II) at the opposite finger, with subsequent conproportionation to Fe(III/II) in the intervening gap as illustrated in Figure 7B.

The second observation relates to the question of maintaining electroneutrality at all points within the film during solid-state voltammetry. We have pointed out in analogous experiments[32] with (sandwiched) films of $([Os(bpy)_2(vpy)_2](ClO_4)_2)_n$ that electroneutrality of the film in the absence of an external supporting electrolyte solution requires an internal supply (which we called the ion budget) of resident, mobile counterions. Thus, in order to generate the gradients of Fe(III/III), Fe(III/II), and Fe(II/II) sites illustrated in Figure 7B (which are drawn asymmetrically in view of the larger D_e values for the Fe(III/III)/Fe(III/II) couple), some ionic species in the Prussian blue film must migrate from one side of the film to the other. Pretreatment of an as-grown Prussian blue film by cycling through the Fe(III/II) → Fe(II/II) reduction in aqueous KNO_3 enhances the solid-state currents that can be observed by ca. 10 times. We associate this effect with the incorporation of K^+ into the film that accompanies electrochemical cycling and a consequently larger ion budget that allows more complete charging of the film.

The third observation relates to the effect of water vapor on the solid-state currents. In experiments conducted in laboratory air, we saw that the solid-state limiting currents appeared to vary directly with the local humidity around the cell. In fact, observation of current through the film was critically dependent on the presence of water vapor in the IDAs bathing environment. If no water vapor, but only dry N_2, is present in the bathing gas, scanning the potential difference ΔE between the IDA finger sets produces no detectable current. More strikingly, if an IDA that has already been polarized at ΔE = 1.5 V in moist air, is placed in a dry N_2 atmosphere, after a short period the current decays to a small value (Figure 7C), yet the IDA fingers *remain* white and golden. The colors persist even when ΔE is returned to zero in an attempt to discharge the IDA. The concentration gradients of Figure 7B are, remarkably, frozen in place by the drying of the Prussian blue film. Thus, the presence of water molecules, probably occupying interstitial sites, is necessary for electron conduction, even in morphologically intact Prussian blue films. This result is analogous to that reported recently[21] on the importance of solvent molecules for intramolecular electron transfer in mixed-valent, oxo-centered, trinuclear iron acetate complexes.

We propose that the importance of the interstitial water is that it acts to solvate internal counterionic species in the Prussian blue film and thereby exerts control over their mobility. Desolvation of the charge-compensating counterions would elevate the barrier associated with local displacements of the counterion accompanying electron hopping that was illustrated above. The results thus form a most interesting contrast. In water-wetted Prussian blue, we deduced from the results in Table I that the local ionic mobility is sufficiently high that D_e for the Fe(III/II) → Fe(II/II) couple is not sensitive to the choice of local cation (among K^+, NH_4^+, Rb^+, and Cs^+). In the absence of water in the solid-state experiment, on the other hand, the local ionic mobility can be made so slow as to control, and close off, the electron-hopping process.

Acknowledgment. This research was supported in part by grants from the National Science Foundation and the Office of Naval Research. Helpful discussions with C. Lundgren (UNC) and SEM micrography by R. Kunz (UNC) are gratefully acknowledged.

Registry No. $Fe_4[Fe(CN)_6]_3$, 14038-43-8; $KFe[Fe(CN)_6]$, 25869-98-1; $NaNO_3$, 7631-99-4; KNO_3, 7757-79-1; NH_4Cl, 12125-02-9; RbCl, 7791-11-9; $RbNO_3$, 13126-12-0; CsCl, 7647-17-8; H_2O vapor, 7732-18-5.

(31) The electrochemistry of the Fe(III/III) state is highly stabilized in moist air relative to films exposed to aqueous electrolytes ($t_{1/2}$ for decay during cyclic voltammetry is ca. 1 min. in KNO_3). Consequently, it proved possible, by the use of a square wave ΔE, to cycle the film between the blue ("off", Fe(III/II)) form and the golden/white form in ambient air a total of 2×10^4 times over 3 days with little change in current (500-ms transient) or color response. The removal of decay–reaction pathways associated with solvents and trace impurities therein may be an unforeseen but general attribute of solid-state voltammetry.

(32) Jernigan, J. C.; Chidsey, C. E. D.; Murray, R. W. *J. Am. Chem. Soc.* **1985**, *107*, 2824.

(33) Some cracking of the film does probably occur upon drying, but this cannot account solely for the above result, since if the film is reexposed to water vapor, currents are again observed, albeit at lower values.

Contribution from the Chemistry Department, Royal Veterinary and Agricultural University, DK-1871 Frederiksberg C, Denmark, and Department of Chemistry, University of California at San Diego, La Jolla, California 92093

Aqueous Solution Photophysics and Photochemistry of Dihalo- and Aquahalobis(ethylenediamine)rhodium(III). Effect of Nonreacting Amine Ligands on Excited-State Halide Dissociation and Excited-State Rearrangement

L. H. Skibsted,*[1] M. P. Hancock,[1] D. Magde,*[2] and D. A. Sexton[2]

Received March 25, 1986

Ligand field excitation of *cis*- and *trans*-$[Rh(en)_2X_2]^+$ (X = Cl, Br) in acidic aqueous solution leads to halide photoaquation producing $[Rh(en)_2(H_2O)X]^{2+}$. Room-temperature phosphorescence lifetimes of the four dihalo complexes in aqueous solution were measured by using a mode-locked laser and time-correlated single-photon detection and found to be about 2 ns in each case. Excited-state halide dissociation and nonradiative deactivation rate constants were evaluated from a combination of the lifetimes and the photoaquation quantum yields. The halide dissociation rate constants range from 1.9×10^8 (*cis*-dichloro) to 2.1×10^7 s^{-1} (*trans*-dibromo) and are in all cases smaller (by a factor of 1.6–15) than the rate constants previously determined for the tetraammine and bis(1,3-propanediamine) analogues. Also described are the syntheses of the dithionate salts of *trans*- and *cis*-$[Rh(en)_2(H_2O)X]^{2+}$, and quantum yields for the cis/trans interconversion of each isomeric pair in aqueous solution at 25 °C are given.

Introduction

Haloaminerhodium(III) complexes undergo efficient and highly stereomobile photosubstitution reactions when irradiated with light of energy matching the multiplicity allowed ligand field transitions. This photoreactivity has been traced to thermally equilibrated lowest energy triplet ligand field states populated by efficient internal conversion and intersystem crossing from the initially populated singlet ligand field states.[3-5] Haloaminerhodium(III) complexes show weak dual photoluminescence, and the longer-lived

(1) Royal Veterinary and Agricultural University.
(2) University of California at San Diego.

(3) Ford, P. C. *Coord. Chem. Rev.* **1982**, *44*, 61.
(4) Ford, P. C.; Wink, D.; DiBenedetto, J. *Prog. Inorg. Chem.* **1983**, *30*, 213.
(5) Skibsted, L. H. *Coord. Chem. Rev.* **1985**, *64*, 343.

0020-1669/87/1326-1708$01.50/0

part of the emission has been identified as phosphorescence from the photoreactive state.[6] A knowledge of photoaquation quantum yields, luminescence quantum yields, and emission lifetimes determined under identical ambient aqueous solution conditions has permitted the calculation of rate constants for ligand dissociation in the photoreactive state and for the radiative and nonradiative deactivation of the same state.[7] Such analyses, which were first accomplished for chloro- and bromopentaamminerhodium(III), have provided a major contribution to the understanding of the excited-state dynamics of this important class of low-spin d^6 metal ion complexes. For the dihalo- and aquahalotetraammine and bis(1,3-propanediamine) complexes, similar analyses have made possible the evaluation of effects due to the stereochemistry and to the reacting and nonreacting ligands on the dynamics of the primary photochemical processes.[8-10] For rhodium(III), ammonia and 1,3-propanediamine have been shown to possess very similar donor properties,[11] and the observed differences between the photochemistry of the tetraammine- and the bis(1,3-propanediamine)rhodium(III) complexes have consequently been attributed to steric rather than electronic factors.[10,12] Ethylenediamine is a significantly stronger σ donor than both ammonia and 1,3-propanediamine,[12,13] and a comparison of the excited-state reaction rate constants for analogous tetraamine complexes of the three amines should facilitate the identification of electronic effects arising from the nonreacting ligands. To contribute to this objective we have undertaken an investigation of the aqueous solution photophysics of the isomeric dibromo- and dichlorobis(ethylenediamine)rhodium(III) complexes in relation to their photochemistry. The photochemistry of these complex ions has been investigated previously with special emphasis on the stereochemical consequences of ligand field excitation and with the use of ^{13}C NMR spectroscopy in combination with optical spectroscopy,[14-17] and the results have formed the basis for theoretical modeling of the excited-state rearrangement processes which follow the primary ligand dissociation process.[18-21]

Experimental Section

Materials. *cis*-$[Rh(en)_2Cl_2]Cl_{0.5}(ClO_4)_{0.5}$ and *cis*-$[Rh(en)_2Br_2]Br\cdot H_2O$ were synthesized as described previously.[22,23] *trans*-$[Rh(en)_2Cl_2]NO_3$ was prepared by a modification of the method of Johnson and Basolo,[24] entailing careful control of the pH of the reaction mixture such that the final pH is 6.5–7.[22] The crude product was reprecipitated from hot 0.01 M HCl by addition of concentrated (~14 M) nitric acid. *trans*-$[Rh(en)_2Cl_2]ClO_4\cdot H_2O$ was precipitated from a hot aqueous solution of the nitrate by addition of an equal volume of 12 M perchloric acid. The product was washed with ice-cold 2 M $HClO_4$, then 96% ethanol, and finally ether and dried in air. Trifluoromethanesulfonic acid ("triflic acid") was obtained from the 3M Co. All other chemicals employed were of analytical or reagent grade and were used without further purification.

Syntheses. I. *trans*-$[Rh(en)_2(H_2O)Cl]S_2O_6\cdot H_2O$. *trans*-$[Rh(en)_2Cl_2]Cl$ is prepared from the nitrate by stirring for 3 h with Amberlite IRA-400 anion-exchange resin in the chloride form (15 mL of resin and 150 mL of water/g of complex) followed by evaporation of the filtered solution to dryness and drying for 2 h at 100 °C in an oven. *trans*-$[Rh(en)_2Cl(OSO_2CF_3)]CF_3SO_3$ is obtained from the latter by the method of Dixon et al.,[25] and after being washed with ether, the yellow product is dried in a desiccator over silica gel. A 1.15-g quantity of the triflato complex is then dissolved with stirring in 0.1 M $HClO_4$ (25 mL). The orange solution is stirred for 1 h at room temperature and then suction-filtered through a fine-porosity sintered-glass funnel. A saturated solution of sodium dithionate (15 mL) is added, and the solution is kept in an ice-bath for $1^1/_2$ h with gentle stirring. The orange-yellow crystals are isolated by filtration and washed with a little ice-cold water, then 96% ethanol, and finally ether. Drying in air gives 0.55 g. The crude product is reprecipitated twice as follows: The product is dissolved on the filter in hot (90–95 °C) water in portions (total dissolution volume ca. 35 mL/g of product), and the solution is filtered. Saturated sodium dithionate solution (30 mL/g of product) and 0.1 M $HClO_4$ (5 mL/g of product) are added to the filtrate and the mixture is then kept in an ice–water bath for 3–4 h with occasional stirring. The crystals are isolated as before, and the final product is dried overnight in a desiccator; yield 0.25 g (27%).

II. *trans*-$[Rh(en)_2Br_2]ClO_4$. *trans*-$[Rh(en)_2Cl_2]Cl$ (see synthesis I; 1.0 g) is dissolved in water (25 mL) with heating, and a hot (~90 °C) solution of sodium bromide (10 g) in 0.1 M HBr (50 mL) is added. The solution is boiled under reflux for 3 h, and a hot (~75 °C), filtered solution of sodium perchlorate hydrate (5 g) in water (15 mL) is added. The solution is allowed to cool to room temperature with occasional agitation and is then kept in an ice–water bath for ca. 1 h. The orange-yellow product is isolated by filtration, washed with 96% ethanol and ether, and dried in air; yield of crude product 1.07 g. The entire reflux and precipitation procedure is then repeated twice more, and the final product is washed with ice-cold 0.1 M $HClO_4$, then 96% ethanol, and ether and dried in air; yield 1.0 g (68%).

III. *trans*-$[Rh(en)_2(H_2O)Br]S_2O_6\cdot H_2O$. This complex is prepared via the intermediate *trans*-$[Rh(en)_2Br(OSO_2CF_3)]CF_3SO_3$ by using a procedure analogous to that for the aquachloro complex (synthesis I): *trans*-$[Rh(en)_2Br_2]Br$ (0.95 g; prepared from the perchlorate (synthesis II) by ion exchange with Amberlite IRA-400 in the bromide form) is stirred in anhydrous triflic acid (5 mL) at 100 °C for $1^1/_4$ h under gentle bubbling with nitrogen gas (hood!). The dark red-brown solution is allowed to cool spontaneously and is then placed in an ice–water bath (with N_2 bubbling maintained). Diethyl ether (25 mL) is added in small portions under vigorous stirring, and the resulting orange-red precipitate is isolated by filtration, washed with ether (2 × 3 mL) and stored in a desiccator; yield of crude triflato complex 1.14 g (93%). The latter product (1.14 g) is stirred at room temperature in 0.1 M $HClO_4$ (25 mL) for 1 h, and saturated sodium dithionate solution (15 mL) is added to the filtered orange solution. The solution is stirred in an ice–water bath for ~$1^1/_2$ h until crystallization begins and is then kept in a refrigerator (~5 °C) for 24 h. The orange-red crystals (0.50 g) are isolated and reprecipitated twice in exactly the same way as the aquachloro complex (synthesis I); yield 0.14 g (15%).

IV. *cis*-$[Rh(en)_2(H_2O)Cl]S_2O_6\cdot H_2O$. *cis*-$[Rh(en)_2Cl_2]Cl_{0.5}(ClO_4)_{0.5}$ (0.724 g, 2.0 mmol) is stirred in the dark at room temperature for 170 h in a solution containing silver(I) perchlorate (3.0 mmol) and 0.1 M $HClO_4$ (5 mL) in water (25 mL). The mixture is filtered through a fine-porosity sintered-glass funnel, and the silver chloride precipitate is washed with water (2 mL). To the combined filtrate and washings is added saturated sodium dithionate solution (10 mL) and then 96% ethanol (10 mL) under vigorous stirring. The solution is kept in a refrigerator (~5 °C) for 5 days, and the pale yellow product is isolated by filtration, washed with 1:1 aqueous ethanol (5 × 2 mL), then 96% ethanol, and ether, and dried briefly in the air. The product is reprecipitated twice by dissolving it at room temperature in water (40 mL/g of complex) and adding a double volume of 96% ethanol to the filtered solution. After the mixture is kept in a refrigerator (~5 °C) overnight, the crystals are isolated and washed as before, and the final product is dried in a desiccator; yield 0.15 g (17%).

V. *cis*-$[Rh(en)_2(H_2O)Br]S_2O_6\cdot H_2O$. This complex is prepared and reprecipitated twice in the same way as the aqua–chloro analogue (synthesis IV), starting with *cis*-$[Rh(en)_2Br_2]Br\cdot H_2O$ (0.962 g, 2.0 mmol), silver(I) perchlorate (4.0 mmol), and 0.1 M $HClO_4$ (5 mL) in water (35 mL) and stirring for 100 h; yield 0.24 g (24%).

Spectra. Electronic absorption spectra were recorded on a Cary Varian 219 spectrophotometer. All of the final products described in

(6) Sexton, D. A.; Ford, P. C.; Magde, D. *J. Phys. Chem.* **1983**, *87*, 197.
(7) Bergkamp, M. A.; Brannon, J.; Magde, D.; Watts, R. J.; Ford, P. C. *J. Am. Chem. Soc.* **1979**, *101*, 4549.
(8) Sexton, D. A.; Skibsted, L. H.; Magde, D.; Ford, P. C. *J. Phys. Chem.* **1982**, *86*, 1758.
(9) Sexton, D. A.; Skibsted, L. H.; Magde, D.; Ford, P. C. *Inorg. Chem.* **1984**, *23*, 4533.
(10) Skibsted, L. H.; Hancock, M. P.; Magde, D.; Sexton, D. A. *Inorg. Chem.* **1984**, *23*, 3735.
(11) Frink, M. F.; Ford, P. C.; Skibsted, L. H. *Acta Chem. Scand., Ser. A* **1984**, *A38*, 795.
(12) Øby, B.; Skibsted, L. H. *Acta Chem. Scand., Ser. A* **1984**, *A38*, 399.
(13) Howland, K.; Skibsted, L. H. *Acta Chem. Scand., Ser. A* **1983**, *A37*, 647.
(14) Muir, M. M.; Huang, W.-L. *Inorg. Chem.* **1973**, *12*, 1831.
(15) Jakse, F. P.; Paukstelis, J. V.; Petersen, J. D. *Inorg. Chim. Acta* **1978**, *27*, 225.
(16) (a) Petersen, J. D.; Jakse, F. P. *Inorg. Chem.* **1979**, *18*, 1818. (b) Clark, S. F.; Petersen, J. D. *Inorg. Chem.* **1979**, *18*, 3394.
(17) Clark, S. F.; Petersen, J. D. *Inorg. Chem.* **1980**, *19*, 2917.
(18) Purcell, K. F.; Clark, S. F.; Petersen, J. D. *Inorg. Chem.* **1980**, *19*, 2183.
(19) Clark, S. F.; Petersen, J. D. *Inorg. Chem.* **1981**, *20*, 280.
(20) Petersen, J. D. *Inorg. Chem.* **1981**, *20*, 3123.
(21) Lee, L.; Clark, S. F.; Petersen, J. D. *Inorg. Chem.* **1985**, *24*, 3558.
(22) Hancock, M. P. *Acta Chem. Scand., Ser. A* **1979**, *A33*, 15.
(23) Hancock, M.; Nielsen, B.; Springborg, J. *Inorg. Synth.* **1986**, *24*, 220.
(24) Johnson, S. A.; Basolo, F. *Inorg. Chem.* **1962**, *1*, 925.
(25) Dixon, N. E.; Lawrance, G. A.; Lay, P. A.; Sargeson, A. M. *Inorg. Chem.* **1984**, *23*, 2940.

Table I. Ligand Field Spectra of Bis(ethylenediamine)rhodium(III) Complexes in 10^{-3} M $HClO_4$

complex	λ_{max} (ϵ)[a]	λ_{min} (ϵ)[a]
trans-$[Rh(en)_2Cl_2]ClO_4 \cdot H_2O$[b]	406 (80), 287 (121)	353 (13), 277 (115)
cis-$[Rn(en)_2Cl_2]Cl_{0.5}(ClO_4)_{0.5}$[c]	351 (200), 294 (195)	320 (131) 272 (126)
trans-$[Rh(en)_2(H_2O)Cl]S_2O_6 \cdot H_2O$[d]	384 (56), 282 (146)	342 (25), 265 (123)
cis-$[Rh(en)_2(H_2O)Cl]S_2O_6 \cdot H_2O$	338 (163), 283 (155)	306 (128), 251 (50)
trans-$[Rh(en)_2Br_2]ClO_4$[e]	428 (115)	367 (13)
cis-$[Rh(en)_2Br_2]Br \cdot H_2O$[f]	366 (254)	335 (174)
trans-$[Rh(en)_2(H_2O)Br]S_2O_6 \cdot H_2O$[g]	460[h] (39), 401 (62)	353 (26)
cis-$[Rh(en)_2(H_2O)Br]S_2O_6 \cdot H_2O$[i]	354 (177)	316 (141)

[a] λ in nm; ϵ in L mol^{-1} cm^{-1}. [b] Ogino and Bailar:[32] λ_{max} (ϵ) = 407 (79), 289 (123) for the chloride salt. [c] Hancock, Nielsen, and Springborg:[23] λ_{max} (ϵ) = 352 (200), 294 (195); λ_{min} (ϵ) = 320 (129), 272 (124). [d] van Eldik, Palmer, Kelm, and Harris:[33] λ_{max} (ϵ) = 384 (56), 283 (143) for the perchlorate salt; cf. ref 15. [e] Ogino and Bailar:[32] λ_{max} (ϵ) = 429 (115) for nitrate salt. [f] Hancock:[22] λ_{max} (ϵ) = 366 (255); λ_{min} (ϵ) = 334 (174); cf. ref 16b. [g] van Eldik, Palmer, Kelm, and Harris:[33] λ_{max} (ϵ) and 465 (31), 396 (58) for the perchlorate salt; cf. ref 16b. [h] Shoulder. [i] Clark and Petersen:[16b] λ_{max} (ϵ) = 358 (133) for the perchlorate salt.

Table II. pK_a Values for Aquahalobis(ethylenediamine)rhodium(III) Complexes in Aqueous 1.0 M $NaClO_4$ at 25 °C[a]

	trans	cis
$[Rh(en)_2(H_2O)Cl]^{2+}$	6.48	7.65
$[Rh(en)_2(H_2O)Br]^{2+}$	6.55	7.59

[a] $pK_a = -\log K_a$. K_a in mol L^{-1}.

Syntheses were reprecipitated such that no change in the spectrum was observed following one further reprecipitation. The spectral characteristics for the purified dihalo and aquahalo complexes are given in Table I and are compared with literature data where these are available.

Analyses. Microanalyses for C, H, N, S, Cl, and Br were carried out by the Microanalytical Laboratory at the H. C. Ørsted Institute, University of Copenhagen, for all the final products described in the section on Syntheses, and satisfactory analyses were obtained in all cases.

pK_a Values. The acid dissociation constants for *trans*- and *cis*-$[Rh(en)_2(H_2O)X]S_2O_6 \cdot H_2O$ (X = Cl or Br) were determined by experimental procedures described previously for the analogous ammonia complexes[26] and are given in Table II.

Photolysis Experiments. Continuous-wave photolyses were carried out in aqueous solution as described previously.[13,27] Temperature control was better than ±1 °C. Light intensities were measured by standard ferrioxalate actinometry.[28] The quantum yields were evaluated from spectral and pH changes (glass electrode measurements) by numerical procedures also described previously.[29]

Emission Lifetime Measurements. Phosphorescence lifetimes were measured by using time-correlated single-photon methods.[30] Although our procedure has been described in previous papers from our laboratories, a number of changes have been made recently and the documentation of previous changes is scattered throughout several papers. Consequently, we outline here the components presently in use.

Photoexcitation is accomplished by using a mode-locked argon ion laser (Spectra Physics Model 2025-05 with optional linear passbank). All the measurements reported here used the 458-nm line. Emission is collected with *f*:2 optics, sent through a 0.5-m monochromator (Spex Model 1870) with a band-pass of 5 nm, and detected with a microchannel plate photomultiplier (Hamamatsu Model 1564U-01) operated at 3200 V. To provide the time reference, a portion of the laser beam is split off with a beamsplitter and sent to a fast PIN photodiode (Hewlett-Packard Model 5082-4203) biased at −90 V. Pulses from both the photomultiplier and the photodiode are amplified (Philips NIM module 774) and sent to a constant-fraction discriminator (EGG/Ortec NIM module 934). Because the reference pulses occur at an 82-MHz repetition rate, a separate gate circuit is used to select only those reference pulses needed for the detected luminescence photons. This was built in-house in a NIM module, following essentially the design of Laws and others.[31] Each detected luminescence photon starts the timing in a time-to-amplitude converter (Canberra NIM module 2044) and the corresponding selected reference pulse stops the timing. The output from the time-to-amplitude converter is amplified in a biased amplifier (Canberra NIM module 1461) and then sent to a multichannel pulse height analyzer (Norland Model 5300), which generates a histogram of the probability of detecting a photon vs. the time delay between the luminescence photon and the reference signal. Such a histogram constitutes precisely the desired luminescence decay profile. Data are transferred to a microcomputer (Heath/Zenith 110) for subsequent processing. Deconvolution by iterative reconvolution is carried out by using a nonlinear least-squares fit to a sum of exponentials with the goodness of fit determined by monitoring the reduced χ^2 parameter, the Durbin–Watson parameter, and the reduced residuals. The instrument response (or "excitation" function) for use in deconvolution was obtained by measuring the Raman scattering of pure water at 550 nm.

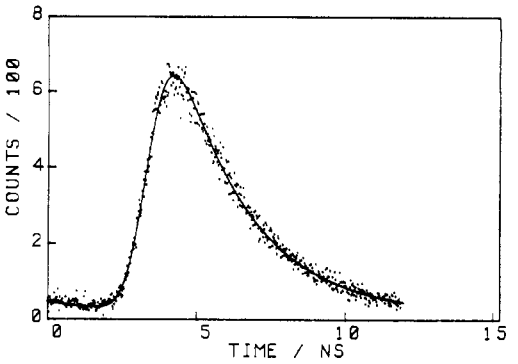

Figure 1. Phosphorescence decay for *trans*-$[Rh(en)_2Br_2]^+$ in aqueous solution. The excitation wavelength was 458 nm. Solid line is the best fit of an exponential convoluted with the excitation (laser pulse) function.

A ratemeter (Canberra NIM module 2081) monitors the luminescence counts per second at all times. To measure luminescence spectra, the output of the ratemeter is plotted on a chart recorder while the monochromator is scanned.

Lifetimes were determined for complexes in aqueous solution at ambient temperature (22 ± 1 °C). Solutions were circulated continuously with a small pump to minimize photolysis. The excitation wavelength was 458 nm, corresponding to the long wavelength tail of the lowest ligand field transition. Concentrations were about 5 mM, which is near the solubility limit. Optical absorbances at the exciting wavelength were about 0.03 for the dichloro complexes and 0.05 for the dibromo complexes. Blanks were run by using the same water supply and all the same glassware.

Results

Emission Lifetimes. The emission spectra of *cis*- and *trans*-$[Rh(en)_2X_2]^+$ (X = Cl, Br) were measured in ambient-temperature aqueous solution. These spectra were very similar to those previously reported[9,10] for the analogous tetraammine and bis(1,3-propanediamine) complexes, and the emission intensities were likewise low with Φ_{em} estimated to be less than 10^{-6}. Low temperature phosphorescence spectra are not available for these particular rhodium(III) complexes. In solution, at room temperature, all show very broad, diffuse phosphorescence in the red. For the dibromo complexes, a broad maximum appears between 700 and 800 nm. For the dichloro complexes, it is impossible to locate a maximum; the phosphorescence merges into the tail of the Raman scattering from the solvent.

Lifetimes were determined for emission in a 5-nm band-pass at 700, 750, and 800 nm. Fresh solutions were prepared and lifetimes remeasured in three independent runs. Figure 1 shows the emission decay curve for *trans*-$[Rh(en)_2Br_2]^+$. The decay

(26) Skibsted, L. H.; Ford, P. C. *Acta Chem. Scand., Ser. A* **1980**, *A34*, 109.
(27) Mønsted, L.; Skibsted, L. H. *Acta Chem. Scand., Ser. A* **1983**, *A37*, 663.
(28) Hatchard, C. G.; Parker, C. A. *Proc. R. Soc. London, A* **1956**, *A235*, 518.
(29) Skibsted, L. H.; Ford, P. C. *Inorg. Chem.* **1980**, *19*, 1828.
(30) Ware, W. R. In *Creation and Detection of the Excited State*; Lamola, A. A., Ed.; Marcel Dekker: New York, 1971; p 213.
(31) Laws, W. R.; Potter, D. W.; Sutherland, J. C. *Rev. Sci. Instrum.* **1984**, *55*, 1564.
(32) Ogino, H.; Bailar, J. C., Jr. *Inorg. Chem.* **1978**, *17*, 1118.

Table III. Quantum Yields for Halide Dissociation and Phosphorescence Lifetimes for Dichloro- and Dibromobis(ethylenediamine)rhodium(III) Ions in Aqueous 10^{-3} M $HClO_4$ at 25 °C

complex ion	Φ_x, mol einstein^{-1}		τ, ns
trans-$[Rh(en)_2Cl_2]^+$	0.056 ± 0.004[a]	(0.061 ± 0.003[e])	2.2 ± 0.4
cis-$[Rh(en)_2Cl_2]^+$	0.47 ± 0.01[b]	(0.43 ± 0.02[e])	2.5 ± 0.4
trans-$[Rh(en)_2Br_2]^+$	0.047 ± 0.001[c]	(0.062 ± 0.005[f])	2.2 ± 0.2
cis-$[Rh(en)_2Br_2]^+$	0.36 ± 0.01[d]	(0.37 ± 0.03[f])	2.5 ± 0.2

[a] λ_{irr} = 366, 405, and 436 nm; a total of six experiments. [b] λ_{irr} = 313, 334, 366, and 405 nm; a total of eight experiments. [c] λ_{irr} = 405 and 436 nm; a total of four experiments. [d] λ_{irr} = 366, 405, and 436 nm; a total of six experiments. [e] Petersen and Jakse.[15] [f] Clark and Petersen.[16]

Table IV. Photoisomerization Quantum Yields[a] for Aquahalobis(ethylenediamine)rhodium(III) Complexes in Aqueous 10^{-3} M $HClO_4$ at 25 °C

	Φ_{ct}	Φ_{tc}
cis-$[Rh(en)_2(H_2O)Cl]^{2+}$ ⇄ *trans*-$[Rh(en)_2(H_2O)Cl]^{2+}$[b]	0.72 ± 0.02	0.013 ± 0.003
cis-$[Rh(en)_2(H_2O)Br]^{2+}$ ⇄ *trans*-$[Rh(en)_2(H_2O)Br]^{2+}$[c]	0.62 ± 0.02[d]	0.007 ± 0.001

[a] Cis to trans photoisomerization quantum yield, Φ_{ct}, and trans to cis photoisomerization quantum yield, Φ_{tc}, in mol einstein^{-1}. [b] λ_{irr} = 313, 334, 366, and 405 nm; a total of eight experiments. [c] λ_{irr} = 334, 366, 405, and 436 nm; a total of six experiments. [d] Clark and Petersen[16] report a value of 0.95 mol einstein^{-1}.

curves could be described by a single exponential function convoluted with the excitation function (see Figure 1). By analogy with the tetraammine and the bis(1,3-propanediamine) complexes,[9,10] the emission was assigned as phosphorescence from the lowest energy ligand field triplet excited state. The lifetimes for the four complexes are given in Table III.

Photochemistry. An investigation of the aqueous solution photochemistry of *cis*- and *trans*-$[Rh(en)_2X_2]^+$ (X = Cl, Br) requires the four complex ions *cis*- and *trans*-$[Rh(en)_2(H_2O)X]^{2+}$ for photoproduct analyses. Although these latter complex ions have all been described previously,[15,16,33] we felt that the described synthetic procedures could be improved, and we have synthesized the trans complexes by the new "triflic acid" method, whereas silver(I)-assisted hydrolysis was employed for the cis isomers. The synthesis and purification was optimized with respect to high purity rather than high yield, in order to obtain accurate spectral data for use in photoproduct analyses. Our observations on the photochemistry of the ethylenediamine complexes differ from those described in the previous reports[16] in the detection of the photoproduct $[Rh(en)_2(H_2O)X]^{2+}$ as a photostationary state, and they can be summarized as follows.

***cis*- and *trans*-$[Rh(en)_2Cl_2]^+$.** Exhaustive photolyses of either isomer in 10^{-3} M $HClO_4$ led to the same photoproduct distribution, and a numerical analysis showed the product to be a mixture of *cis*- and *trans*-$[Rh(en)_2(H_2O)Cl]^{2+}$ in a photostationary state. This latter point was proven by direct irradiation of solutions of either isomer of $[Rh(en)_2(H_2O)Cl]^{2+}$. The quantum yields for the interconversion of the aquachloro complexes in 10^{-3} M $HClO_4$, which were found to be independent of the wavelength of irradiation, are given in Table IV. The cis/trans ratio in the photostationary state calculated from the quantum yields of Table IV and the molar absorptivities of *cis*- and *trans*-$[Rh(en)_2(H_2O)Cl]^{2+}$ at the wavelength of irradiation agreed with the isomer ratio calculated from the spectra of exhaustively photolyzed solutions. For 405-nm irradiation, the photostationary state corresponds to 95.4% trans, whereas for 366-nm irradiation, the photostationary state is shifted almost completely to trans (99.3%), owing to a higher ϵ_{366} value for *cis*- than for *trans*-$[Rh(en)_2(H_2O)Cl]^{2+}$. The quantum yields for chloride photoaquation in the dichloro complexes calculated from spectral data[10,29] are given in Table III. Thermal reactions were found to be of no significance for any of the complex ions investigated under the experimental conditions used, and no amine photoaquation could be detected.

***cis*- and *trans*-$[Rh(en)_2Br_2]^+$.** The photoproduct formed from either isomer of the dibromo complexes was found to be $[Rh(en)_2(H_2O)Br]^{2+}$ in a cis/trans photostationary state, with an even stronger preference for the trans geometry than in the case of the chloro analogues (e.g. 98.8% trans for 405-nm irradiation). This was confirmed by the relative magnitude of the quantum yields for interconversion of *cis*- and *trans*-$[Rh(en)_2(H_2O)Br]^{2+}$ (determined by irradiation of solutions of the dithionate salt of either isomer), which are given in Table IV. The bromide photoaquation quantum yields for *cis*- and *trans*-$[Rh(en)_2Br_2]^+$ determined[10,29] in the present study are given in Table III.

Discussion

Ligand field excitation of haloaminerhodium(III) complexes produces the lowest energy triplet state with quantum yield close to unity (cf. ref 3, 4). This triplet state, which is the photoreactive state, emits weak phosphorescence, and the quantum yields for the various triplet deactivation processes may be described by

$$\Phi_i = \Phi_{isc}\frac{k_i}{k_x + k_r + k_n} = \Phi_{isc}k_i\tau$$

where k_x is the excited-state rate constant for ligand substitutions, k_r and k_n are the rate constants for radiative and nonradiative deactivation, respectively, Φ_{isc} is the intersystem crossing yield, and τ is the phosphorescence lifetime.[7] The intersystem crossing yield is close to unity ($\Phi_{isc} \sim 1$) and the phosphorescenee efficiency is small ($\Phi_r < 10^{-6}$), and consequently $k_r << k_x + k_n$, allowing the evaluation of k_x and k_n from halide-substitution quantum yields and lifetimes measured under identical conditions (see footnotes to Table V). The rate constants determined for *cis*- and *trans*-$[Rh(en)_2X_2]^+$ (X = Cl, Br) are summarized in Table V together with those for the tetraammine and bis(1,3-propanediamine) analogues determined previously.[9,10]

The *nonradiative deactivation* rate constants are very similar for the dihalotetraamine complexes investigated, and range from 2.1×10^8 s^{-1} for *cis*-$[Rh(en)_2Cl_2]^+$ to 1.4×10^9 s^{-1} for *trans*-$[Rh(tn)_2Br_2]^+$. However, the dibromo complexes show consistently faster radiationless deactivation than their chloro analogues, as also seen for the perprotio and perdeuterio halopentaammine-rhodium(III) complexes,[7] and for each isomer pair, the radiationless deactivation is marginally faster for the trans geometry in most cases, in agreement with the energy-gap law.[34]

The *excited-state halide substitution* rate constants have been identified as ligand dissociation rate constants,[5,27,35] and are consistently smaller for the ethylenediamine complexes than for both the ammonia and the 1,3-propanediamine analogues (Table V). For the ammonia and the ethylenediamine complexes, the relative halide dissociation rates are independent of whether the leaving ligand is chloride or bromide. However, the rates depend on the stereochemistry, as may be seen from the rate constant ratios: for the trans isomers, $k_{Cl}^{en}/k_{Cl}^{NH_3} = k_{Br}^{en}/k_{Br}^{NH_3} = 0.3$; for the cis isomers, $k_{Cl}^{en}/k_{Cl}^{NH_3} = k_{Br}^{en}/k_{Br}^{NH_3} = 0.6$. If steric factors were the more important in determining the difference in reactivities, then the ratio between the dissociation rates should depend not only on the nature of the amine but also on the bulkiness of the halide, and the observed difference between the halide dissociation rates for the ammonia and the ethylenediamine complexes is thus a consequence of the bonding pattern in the triplet excited state (electronic factors) rather than of steric factors. For the three amine series, the lability of a halide in the excited state is higher for the cis than for the trans stereochemistry, and the fact that halide dissociation rates are accelerated twice as much for the trans as for the cis complexes for both chloride and bromide upon changing ammonia for ethylenediamine identifies the cis ligands

(33) van Eldik, R.; Palmer, D. A.; Kelm, H.; Harris, G. M. *Inorg. Chem.* **1980**, *19*, 3679.

(34) The lowest energy triplet state for the trans species should be closer in energy to the ground state (parallels spin-allowed states), making relaxation to the ground state more efficient for the trans isomer because of the energy-gap law. We thank a reviewer for this comment.

(35) Mønsted, L.; Skibsted, L. H. *Acta Chem. Scand. Ser. A* **1984**, *A38*, 535.

Table V. Rate Constants (s^{-1}) for Halide Dissociation[a] and Nonradiative[b] Deactivation from the Lowest Energy Ligand Field Excited State for Dichloro- and Dibromotetraaminerhodium(III) Complexes in Dilute Aqueous Solution at 25 °C

	tetraammine[c]		bis(ethylenediamine)[d]		bis(1,3-propanediamine)[e]	
complex	k_x^f	k_n	k_x^f	k_n	k_x^f	k_n
trans-$[RhA_4Cl_2]^+$	$(8 \pm 1) \times 10^7$	$(5 \pm 1) \times 10^8$	$(2.5 \pm 0.5) \times 10^7$	$(4.3 \pm 0.8) \times 10^8$	$(5.7 \pm 0.4) \times 10^7$	$(6.6 \pm 0.5) \times 10^8$
cis-$[RhA_4Cl_2]^+$	$(3.0 \pm 0.6) \times 10^8$	$(5 \pm 2) \times 10^8$	$(1.9 \pm 0.3) \times 10^8$	$(2.1 \pm 0.4) \times 10^8$	$(6.2 \pm 0.6) \times 10^8$	$(4.9 \pm 1.2) \times 10^8$
trans-$[RhA_4Br_2]^+$	$(6.3 \pm 0.7) \times 10^7$	$(6.0 \pm 0.5) \times 10^8$	$(2.1 \pm 0.2) \times 10^7$	$(4.3 \pm 0.4) \times 10^8$	$(8.2 \pm 1.0) \times 10^7$	$(1.4 \pm 0.2) \times 10^9$
cis-$[RhA_4Br_2]^+$	$(2.4 \pm 0.3) \times 10^8$	$(7 \pm 1) \times 10^8$	$(1.4 \pm 0.1) \times 10^8$	$(2.6 \pm 0.3) \times 10^8$	$(2.1 \pm 0.4) \times 10^9$	$(1.2 \pm 0.7) \times 10^9$

[a] Calculated from $k_x = \Phi_x \tau^{-1}$. [b] Calculated from $k_n = \tau^{-1} - k_x$. [c] $A_4 = (NH_3)_4$.[9] [d] $A_4 = (en)_2$; this work. [e] $A_4 = (tn)_2$.[10] [f] k_x is the halide dissociation rate constant (X = Cl, Br).

Table VI. Φ_{tc}/Φ_{ct} for Diaqua- and Aquahalotetraaminerhodium(III) Complexes in Dilute Aqueous Solution at 25 °C

complex	tetra-ammine[a]	bis(ethylene-diamine)[b]	bis(1,3-propane-diamine)[c]
$[RhA_4(H_2O)_2]^{3+}$	0.11	<0.007	0.34
$[RhA_4(H_2O)Cl]^{2+}$	0.12	0.018	0.14
$[RhA_4(H_2O)Br]^{2+}$	0.039	0.011	0.086

[a] $A_4 = (NH_3)_4$.[27,35] [b] $A_4 = (en)_2$; this work and ref 13. [c] $A_4 = (tn)_2$.[10,12]

as being the more important in determining the relative halide dissociation rates.

In the case of thermal (ground-state) reactions,[36] *cis*-dihalo complexes likewise react faster than the analogous *trans*-dihalo complexes, and for a given halide and stereochemistry, the ammonia complexes also react faster than the analogous ethylenediamine and 1,3-propanediamine complexes, as illustrated by the chloride/bromide interchange reaction

$$trans\text{-}RhA_4Cl_2^+ + Br^- \rightarrow trans\text{-}RhA_4ClBr^+ + Cl^-$$

for which the relative rates at 80 °C are, for $A_4 = (NH_3)_4$, $(en)_2$, and $(tn)_2$, 1:0.5:0.4.[37] Our present observations on the triplet excited-state reactivities show, when compared to the ground-state reactivities, that different activation processes are operative in the ground state and in the excited state. The ground-state reactivities can be correlated with the hydrophobicity of the nonreacting amine (i.e. less efficient transition-state solvation of the larger complexes), whereas the excited-state reactivity can be correlated with the donor strength of the amine, which is consistent with a higher degree of dissociative activation for the latter processes.

The excited-state rearrangement following ligand dissociation has been shown to attain thermal equilibrium prior to deactivation[35]

$$apical\text{-}RhA_4X^{2+*} \overset{K_s}{\rightleftharpoons} basal\text{-}RhA_4X^{2+*}$$

and the Φ_{tc}/Φ_{ct} ratios of Table VI represent estimates of the excited state basal/apical preferences. The relative energies of the apical and basal isomers have been estimated from angular overlap calculations,[18,38,39] and for a given ligand X, the trans preference is expected to decrease with decreasing σ-donor capability of the amine.[5] Spectral data for $[RhA_4X_2]^+$ show that ethylenediamine consistently has a stronger field strength than ammonia or 1,3-propanediamine,[10,12,13] with the latter two amines showing very similar σ-donor properties: $\sigma_{tn} \sim \sigma_{NH_3} < \sigma_{en}$. The increasing trans preference along the series tn < NH_3 < en validates the angular overlap calculation and for 1,3-propanediamine and ammonia suggests the former to be the weaker ligand, as also concluded from measurements of low-temperature emission energies.[11]

Compared to ground-state ligand substitution reactions, the excited-state ligand dissociation reactions are very fast processes (rate acceleration by a factor of 10^{14} or more[7]), and their rate approaches that suggested for intersystem crossing processes.[6,40] However, the rate data obtained for the present series of dihalotetraaminerhodium(III) complexes show that certain patterns of reactivity can be recognized and accounted for in terms of electronic and steric effects similar to those normally invoked to rationalize ground-state (thermal) chemistry. The internal consistency of these conclusions reinforces our confidence in the simple kinetic model used to interpret photophysical and photochemical data and suggests that recent molecular orbital theories can account for major features of rhodium(III) photochemistry.

Acknowledgment. This research was supported by grants from the Danish Natural Science Research Council (to L.H.S.) and the National Science Foundation (No. CHE-8409642 to D.M.). Some of the laser apparatus was provided by a grant from the National Institutes of Health. The rhodium used in these studies was provided on loan from Johnson Matthey. The authors thank Bodil Øby for technical assistance.

Registry No. *trans*-$[Rh(en)_2Cl_2]ClO_4$, 41367-59-3; *cis*-$[Rh(en)_2Cl_2]Cl$, 15444-62-9; *trans*-$[Rh(en)_2(H_2O)Cl]S_2O_6$, 107890-71-1; *cis*-$[Rh(en)_2(H_2O)Cl]S_2O_6$, 107890-72-2; *trans*-$[Rh(en)_2Br_2]ClO_4$, 55683-56-2; *cis*-$[Rh(en)_2Br_2]Br$, 65761-17-3; *trans*-$[Rh(en)_2(H_2O)Br]S_2O_6$, 107890-73-3; *cis*-$[Rh(en)_2(H_2O)Br]S_2O_6$, 107890-74-4; *trans*-$[Rh(en)_2Cl_2]^+$, 18539-17-8; *cis*-$[Rh(en)_2Cl_2]^+$, 24444-43-7; *trans*-$[Rh(en)_2Br_2]^+$, 24444-44-8; *cis*-$[Rh(en)_2Br_2]^+$, 53368-52-8; *cis*-$[Rh(en)_2(H_2O)Cl]^{2+}$, 53368-47-1; *cis*-$[Rh(en)_2(H_2O)Br]^{2+}$, 53368-48-2; *trans*-$[Rh(en)_2(H_2O)Cl]^{2+}$, 15337-41-4; *trans*-$[Rh(en)_2(H_2O)Br]^{2+}$, 15337-42-5; *trans*-$[Rh(en)_2Cl(OSO_2CF_3)]CF_3SO_3$, 90065-97-7; *trans*-$[Rh(en)_2Cl_2]NO_3$, 15529-88-1; *trans*-$[Rh(en)_2Br(OSO_2CF_3)]CF_3SO_3$, 107890-76-6.

(36) Basolo, F.; Pearson, R. G. *Mechanisms of Inorganic Reactions*; 2nd ed.; Wiley: New York, 1967, Chapter 3.
(37) Thirst, A. J.; Vaughan, D. H. *J. Inorg. Nucl. Chem.* **1981**, *43*, 2889.
(38) Vanquickenborne, L. G.; Ceulemans, A. *Inorg. Chem.* **1978**, *17*, 2730.
(39) Vanquickenborne, L. G.; Ceulemans, A. *Inorg. Chem.* **1981**, *20*, 110.
(40) Kobayashi, T.; Okashi, Y. *Chem. Phys. Lett.* **1982**, *86*, 289.